

Correction

Correction: Orun et al. Stabilizing DNA–Protein Co-Crystals via Intra-Crystal Chemical Ligation of the DNA. *Crystals* 2022, 12, 49

Abigail R. Orun ¹, Sara Dmytriw ², Ananya Vajapayajula ² and Christopher D. Snow ^{1,2,*}

¹ Department of Chemistry, Colorado State University, 1301 Center Ave, Fort Collins, CO 80523, USA; abby.orun@vumc.org

² Department of Chemical and Biological Engineering, Colorado State University, 1370 Campus Delivery, Fort Collins, CO 80523, USA; sara.dmytriw@rams.colostate.edu (S.D.); avajapayajula3@gatech.edu (A.V.)

* Correspondence: christopher.snow@colostate.edu

In the publication [1], gel electrophoresis DNA bands were interpreted erroneously as double-stranded DNA (dsDNA). The TBE-urea gel electrophoresis denatured the DNA, and the bands are single-stranded DNA (ssDNA). The authors present a correction to the gel interpretation in the ligation simulations, ligation product, and probability calculations and figure labels. The overarching findings of the crystal ligation have not changed, although the overall ligation yields are higher than originally reported.

Updated ligation calculation and modeling scripts are published on Zenodo [2].

Error in Figure

A corrected Figure 4 shows ssDNA bands labelled with nucleotides ('nt').

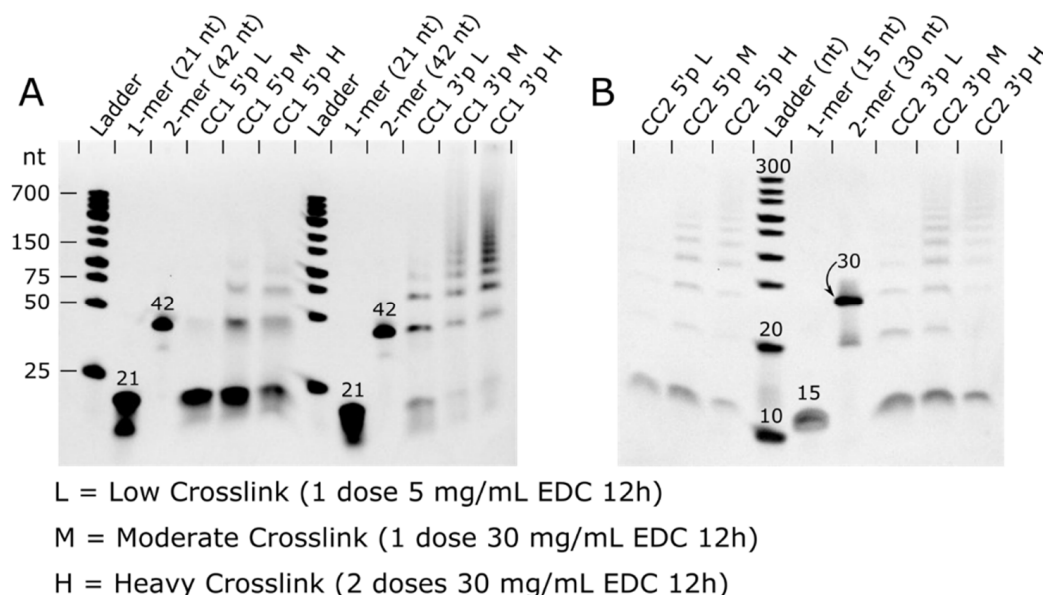


Figure 4. TBE-urea gels of: (A) CC1; and (B) CC2 chemical ligation. In both co-crystals, additional ligation was achieved with increased EDC concentration and a second EDC dose. (A) A 10% TBE-urea gel of CC1 illustrating a much-improved ligation product distribution for 3' vs. 5' phosphates. (B) A 15% TBE-urea gel of CC2 illustrating a modestly improved ligation product distribution for 3' vs. 5' phosphates. Assigned band sizes are given in nt.

Correction in Section 3.2

The text, equations and values in Section 3.2 were updated to reflect ssDNA. Specifically, the probabilities were changed from the probability of a double-stranded break to the



Citation: Orun, A.R.; Dmytriw, S.; Vajapayajula, A.; Snow, C.D.

Correction: Orun et al. Stabilizing DNA–Protein Co-Crystals via Intra-Crystal Chemical Ligation of the DNA. *Crystals* 2022, 12, 49. *Crystals* 2023, 13, 675. <https://doi.org/10.3390/cryst13040675>

Received: 14 March 2023

Accepted: 21 March 2023

Published: 14 April 2023



Copyright: © 2023 by the authors. Licensee MDPI, Basel, Switzerland. This article is an open access article distributed under the terms and conditions of the Creative Commons Attribution (CC BY) license (<https://creativecommons.org/licenses/by/4.0/>).

probability of a single-stranded break. A corrected Table 4 shows the updated probability terminologies and calculated values.

3.2. Ligation Model Compared to Experimental Co-Crystal Ligation

The ligation product distributions we experimentally obtained should shed light on the stochastic process of ligation. Using a destructive assay, densitometric analysis of electrophoresis results on ssDNA recovered from dissolved crystals, we quantified the population ratio of bands assigned to non-modified DNA blocks as well as fused 2-mer, 3-mer, etc. For selected gels, we also obtained TapeStation results (Figure S1). The relative population of the end-product distribution was fairly consistent for gel band populations measured with TBE-urea gels in ImageJ compared to the automated TapeStation analysis (Figure S1).

Next, we sought to calculate a global performance metric for the ligation yield, P_{LIG} , as the fraction of all possible DNA–DNA nick sites throughout a crystal that were ligated. To quantify the ligation yield throughout an entire crystal, we analyzed the implications of the final DNA product distribution recovered after the crystal is dissolved and the protein components are removed. If we count the number of DNA oligos of each length (n_i) that were present in the crystal, and we ignore edge effects, we can estimate the total number of single-stranded breaks (SSB) as $N_{SSB} = \sum_i n_i$. For the same crystal, the estimated total number of original single-strand breaks (regardless of final ligation status) would be $N_{JXN} = \sum_i i \cdot n_i$. For example, adding a single fused 3-mer to the crystal increases the SSB tally by one, but increases the tally of all possible junctions by three. Then, to compute the total probability of encountering SSB, we calculate:

$$P_{SSB} = \frac{N_{SSB}}{N_{JXN}} = \frac{\sum_i n_i}{\sum_i i \cdot n_i} = \frac{\frac{\sum_i n_i}{\sum_i n_i}}{\frac{\sum_i i \cdot n_i}{\sum_i n_i}} = \frac{1}{\sum_i i \cdot x_i} \quad (1)$$

In the final equation, x_i is the mole fraction for i -mer oligos. Therefore, to estimate the P_{SSB} , we can use estimated mole fractions from electrophoresis and densitometry (Figures S2 and 4 and Table 4). Accurately calculating P_{SSB} does require including the small mole fractions for higher-order products (Table S3) since longer products contribute proportionally more to $\sum_i i \cdot x_i$. To estimate the uncertainty in each P_{SSB} , we used 500 numerical trials in which random noise was added to $i \cdot x_i$ to mimic the densitometry measurement error. We used noise comparable to $i \cdot x_i$ for the highest-order ligation products (normal variate with standard deviation 0.03), such that the smallest $i \cdot x_i$ values would regularly fall to 0 after the addition of random noise.

Given the probability of encountering a single-stranded break in the crystal (P_{SSB}), it is trivial to calculate the probability of each terminal phosphate having undergone ligation (P_{LIG}), since $P_{LIG} = 1 - P_{SSB}$. In the context of the random ligation model (RLM), ligation events throughout the crystal are independent and occur with equal probability at all nick sites. This is a physically plausible model if the intra-crystal transport rate for EDC exceeds the rate of reaction. Therefore, the incidence of double-stranded breaks within the crystal should occur with the joint probability of independent events, $P_{DSB} = (P_{SSB})^2$.

This analysis of the electrophoresis experiments suggests that ~75% of the terminal phosphates within the most thoroughly crosslinked CC1-3P crystal have undergone ligation. Furthermore, ~94% of the DNA–DNA junctions in this crystal had at least one ligated chain. The similarity in ligation yield for the medium- and high-dose cases leads to an important question. What factors are limiting the yield? Incomplete ligation could result if a random population of terminal phosphates are missing, or otherwise incapable of on-target ligation. We used simulations to verify that the predicted RLM product ratio did not change when we postulated that a random subset of nick sites is incapable of ligation. This makes sense because junctions that are randomly selected to be incapable of ligation are functionally equivalent to sites that are randomly selected to be ligated last.

It may also be possible that ligating one phosphate at a DNA–DNA junction would negatively affect neighboring ligation probabilities. However, evidence for such allostery is lacking. Instead, the observed product distributions for CC1 ligation outcomes (Table 4), were close to the distributions predicted by the RLM (Figure S12). One small but consistent deviation from the RLM was a lower 2-mer, and higher 3-mer population than predicted. This observation seems to preclude the simplest negative allostery scenario (where one ligation event would reduce the probability at flanking sites). We cannot rule out the possibility that this discrepancy is an artifact associated with the gel electrophoresis densitometry.

Table 4. Distribution of DNA block sizes as a function of crosslinking protocol and 3' vs. 5' terminal phosphates. The data shown correspond with the gel lanes in Figure 4. The crosslinking protocols low, medium, and high were 1 dose of 5 mg/mL EDC for 12 h, 1 dose of 30 mg/mL EDC for 12 h, and 2 doses of 30 mg/mL EDC for 12 h each, respectively. The values in this table are weighted so that the DNA length and dye intensity contributes to the final value. Unweighted values are found in Table S2. The full table, including estimated mole fractions for higher-order products, is found in Table S3. P_{SSB} , P_{LIG} , and P_{DSB} were calculated for each crosslinked crystal sample. Uncertainties are standard deviations in derived quantities after 500 trials in which noise (standard deviation 0.03) is introduced into relative band intensities.

Parent Crystal	CC1-3'P	CC1-3'P	CC1-3'P	CC1-5'P	CC1-5'P	CC1-5'P
Crosslinking Protocol	low	medium	high	low	medium	high
DNA block size	[%]	[%]	[%]	[%]	[%]	[%]
1	58.7	30.0	24.9	98.6	91.6	82.1
2	18.7	16.8	14.9	1.4	7.3	9.9
3	15.2	15.3	15.6		1.0	6.3
4	5.0	11.0	11.0		0.2	1.5
5	2.4	6.3	8.4			0.2
6		6.5	6.9			
7		4.4	5.8			
8 and above		9.7	12.5			
P_{SSB} *	0.58 ± 0.01	0.28 ± 0.01	0.25 ± 0.01	0.99 ± 0.01	0.91 ± 0.02	0.78 ± 0.02
$P_{LIG} = 1 - P_{SSB}$	0.42 ± 0.01	0.72 ± 0.01	0.75 ± 0.01	0.01 ± 0.01	0.09 ± 0.02	0.22 ± 0.02
$P_{DSB} = (P_{SSB})^2$	0.33 ± 0.01	0.08 ± 0.01	0.06 ± 0.005	0.97 ± 0.02	0.83 ± 0.04	0.61 ± 0.03
Parent Crystal	CC2-3'P	CC2-3'P	CC2-3'P	CC2-5'P	CC2-5'P	CC2-5'P
Crosslinking Protocol	low	medium	high	low	medium	high
DNA block size	[%]	[%]	[%]	[%]	[%]	[%]
1	94.4	80.3	74.4	96.9	84.8	72.2
2	2.6	4.8	3.3	1.2	5.6	3.1
3	1.5	4.5	4.4	1.9	4.9	7.7
4	0.8	3.6	3.7		2.6	5.2
5	0.7	2.5	2.9		1.1	2.9
6		1.3	2.9		1.0	2.7
7		1.3	2.3			1.9
8 and above		1.7	6.1			4.3
P_{SSB} *	0.90 ± 0.03	0.61 ± 0.03	0.45 ± 0.02	0.95 ± 0.02	0.75 ± 0.02	0.48 ± 0.01
$P_{LIG} = 1 - P_{SSB}$	0.10 ± 0.03	0.39 ± 0.03	0.55 ± 0.02	0.05 ± 0.02	0.25 ± 0.02	0.52 ± 0.01
$P_{DSB} = (P_{SSB})^2$	0.82 ± 0.05	0.37 ± 0.05	0.20 ± 0.02	0.91 ± 0.04	0.57 ± 0.03	0.23 ± 0.01

* Calculated from experimental mole fractions per Equation (1). Other probabilities are calculated using the formulas shown. The double-strand break probability estimate makes the assumption that ligation probability of both nicks at the same DNA–DNA junction are the same and independent. Uncertainty (Δ) propagation: $P_{DSB} = \sqrt{(2 \cdot P_{SSB} \cdot \Delta P_{SSB})^2}$.

The CC2 ligation outcomes (Table 4) were significantly less consistent with distributions predicted by the RLM. Once more, the 3-mer population was often higher than

expected, frequently exceeding the 2-mer population (which never happens in the RLM). This effect also seemed to extend to anomalously common 4-mers. A more striking divergence from the RLM prediction was the high population of non-ligated 1-mer blocks. Regardless of the RLM fit, the significant difference between the 1-mer mole fractions and the P_{SSB} values obtained from all the mole fractions strongly implicates that the RLM is lacking.

To investigate, we tested biased ligation model simulations. One possible explanation is that the ligation outcomes were driven partially by kinetics and molecular transport phenomena. Hypothetically, ligation sites near the crystal exterior might be more likely to be ligated than possible sites near the crystal center since reactive molecules must traverse the outer layers to react the interior. To determine the likely implications of this scenario, we conducted biased random ligation simulations (Protocol S3) that increased the probability of ligation events near the surface, decreased the probability at the center, and terminated the random ligation process at a set P_{SSB} threshold. Perhaps counterintuitively, this spatial bias increased the predicted 1-mer mole fraction. A high 1-mer fraction is partially consistent with the observed product distribution for CC2. The overall lower ligation yield achieved for CC2 crystals compared to CC1 is also consistent with the hypothesis that the CC2 crystal interior is systematically under-ligated. Alternately, it could be the case that one of the two symmetry-distinct nick sites in the CC2 lattice has a significantly lower ligation yield, and therefore one of the two DNA oligos will be over-represented in the 1-mer population.

Correction in Discussion Section

In the Discussion, the authors updated the ligation product yields.

Global analysis of the ligation product distribution suggested that the most thoroughly crosslinked CC1 crystals feature ligation of approximately 75% of all possible ligation sites, covalently linking about 94% of the DNA–DNA junctions through one or more covalent bond. Ligation was corroborated by single-crystal XRD where we could directly observe ligation in electron density omit maps (Figure 5).

Supplemental Information Correction

The supplemental information was updated to reflect the ssDNA interpretation. The updated information is in Figure S12, Table S3, and Protocols S2 and S3.

Correction in Data Availability Statement

In the Data Availability Statement, the authors updated the link to Zenodo data and scripts.

Data Availability Statement: The data presented in this study are openly available in Zenodo at <https://doi.org/10.5281/ZENODO.7667968> (accessed on 1 March 2023).

Correction in Acknowledgments

In the Acknowledgements, the authors would like to express gratitude to Shing Ho for identifying a flaw in the interpretations of an earlier version of our analysis.

Acknowledgments: Hataichanok (Mam) Scherman, Director of the Histone Source at Colorado State University for the expression and purification of the RepE54 transcription factor and the purification of E2F8 transcription factor. Shing Ho for advice and identifying a flaw in the interpretation of an earlier version of our analysis. Mark Stenglein and Mikaela Samsel at the Next Generation Sequencing Facility at Colorado State University for TapeStation analysis. Jay Nix at the ALS Beamline 4.2.2 for extensive support of the XRD data collection. The Taipale Lab for their CC2 protein plasmid donation. Thaddaus Huber for cloning expertise and PSB3 plasmid.

The authors apologize for any inconvenience caused and state that the scientific conclusions are unaffected. The original publication has also been updated.

References

1. Orun, A.R.; Dmytriw, S.; Vajapayajula, A.; Snow, C.D. Stabilizing DNA–Protein Co-Crystals via Intra-Crystal Chemical Ligation of the DNA. *Crystals* **2022**, *12*, 49. [[CrossRef](#)]
2. Ward, A.R.; Snow, C.D. *Scripts for Modeling Chemical Ligation of DNA Junctions within Biomolecular Crystals*; Zenodo: Geneva, Switzerland, 2021; Version 2. [[CrossRef](#)]

Disclaimer/Publisher’s Note: The statements, opinions and data contained in all publications are solely those of the individual author(s) and contributor(s) and not of MDPI and/or the editor(s). MDPI and/or the editor(s) disclaim responsibility for any injury to people or property resulting from any ideas, methods, instructions or products referred to in the content.